

2009

Regulation of Intracellular Calcium Concentration by Nanosecond Pulsed Electric Fields

Shaka S. Scarlett
Old Dominion University


Jody A. White
Old Dominion University

Peter F. Blackmore

Karl H. Schoenbach
Old Dominion University, kschoenb@odu.edu

Juergen Kolb
Old Dominion University, jkolb@odu.edu

Follow this and additional works at: https://digitalcommons.odu.edu/bioelectrics_pubs

 Part of the [Biochemistry Commons](#), [Biomedical Engineering and Bioengineering Commons](#), [Biophysics Commons](#), and the [Molecular Biology Commons](#)

Repository Citation

Scarlett, Shaka S.; White, Jody A.; Blackmore, Peter F.; Schoenbach, Karl H.; and Kolb, Juergen, "Regulation of Intracellular Calcium Concentration by Nanosecond Pulsed Electric Fields" (2009). *Bioelectrics Publications*. 185.
https://digitalcommons.odu.edu/bioelectrics_pubs/185

Original Publication Citation

Scarlett, S. S., White, J. A., Blackmore, P. F., Schoenbach, K. H., & Kolb, J. F. (2009). Regulation of intracellular calcium concentration by nanosecond pulsed electric fields. *Biochimica et Biophysica Acta*, 1788(5), 1168-1175. doi:10.1016/j.bbamem.2009.02.006



Regulation of intracellular calcium concentration by nanosecond pulsed electric fields

Shaka S. Scarlett^a, Jody A. White^a, Peter F. Blackmore^b, Karl H. Schoenbach^a, Juergen F. Kolb^{a,*}

^a Frank Reidy Research Center for Bioelectrics, Old Dominion University, Norfolk, VA, USA

^b Department of Physiological Sciences, Eastern Virginia Medical School, Norfolk, VA, USA

ARTICLE INFO

Article history:

Received 2 November 2008

Received in revised form 14 January 2009

Accepted 2 February 2009

Available online 20 February 2009

Keywords:

nsPEF

Membrane poration

Intracellular Ca^{2+}

Jurkat cell

Fluo-4

Brefeldin A BODIPY®

ABSTRACT

Changes in $[\text{Ca}^{2+}]_i$ response of individual Jurkat cells to nanosecond pulsed electric fields (nsPEFs) of 60 ns and field strengths of 25, 50, and 100 kV/cm were investigated. The magnitude of the nsPEF-induced rise in $[\text{Ca}^{2+}]_i$ was dependent on the electric field strength. With 25 and 50 kV/cm, the $[\text{Ca}^{2+}]_i$ response was due to the release of Ca^{2+} from intracellular stores and occurred in less than 18 ms. With 100 kV/cm, the increase in $[\text{Ca}^{2+}]_i$ was due to both internal release and to influx across the plasma membrane. Spontaneous changes in $[\text{Ca}^{2+}]_i$ exhibited a more gradual increase over several seconds. The initial, pulse-induced $[\text{Ca}^{2+}]_i$ response initiates at the poles of the cell with respect to electrode placement and co-localizes with the endoplasmic reticulum. The results suggest that nsPEFs target both the plasma membrane and subcellular membranes and that one of the mechanisms for Ca^{2+} release may be due to nanopore formation in the endoplasmic reticulum.

© 2009 Elsevier B.V. All rights reserved.

1. Introduction

Nanosecond pulsed electric fields (nsPEFs) have demonstrated the ability to induce a variety of responses in cells such as increases in intracellular free Ca^{2+} ($[\text{Ca}^{2+}]_i$), caspase activation, phosphatidylserine (PS) externalization, and DNA damage [1–7]. Classical electroporation uses field strengths of several hundred volts per centimeter for microsecond to millisecond durations to allow passage of normally non-permeable molecules across the plasma membrane. In comparison, nsPEF-exposures use much higher field strengths of several hundred kV/cm for durations often shorter or on the order of the charging time of the plasma membrane (typically 100–300 ns). The rise time of conventional electroporation pulses alone is often longer than the entire pulse duration of nsPEFs. For long pulse durations, ions accumulate along the plasma membrane, and a counterfield develops inside the cell that effectively shields the organelles from further exposure to the applied electric field. As a result, only the outer membrane is affected by the prolonged exposure and pores form once a cell-characteristic threshold voltage is reached [8–10]. The time constant for the charging process depends on cell size and conductivity of the suspension media [11,12]. For a spherical cell, 10 μm in diameter, suspended in a physiological buffer, it is on the order of 75 ns. Conversely, within the short duration of nsPEF exposures, organelle membranes will be affected in the same way as the outer cell membrane. For the high electric field strengths applied with nsPEFs, transmembrane voltages reach values of more than 1 V

during the exposure and pore formation is also likely along internal membranes [13]. In addition to this direct effect on membrane structure, the intense fields allegedly affect voltage-gated channels and other protein structures in the membrane [14,15]. Ca^{2+} stores, such as in the endoplasmic reticulum (ER) and mitochondria, are presumably targeted by the same mechanisms, causing the release of Ca^{2+} into the cytosol [16]. Therefore, changes in $[\text{Ca}^{2+}]_i$ are among the first physiological responses of the cell to nsPEFs.

In the present study, we explored changes in $[\text{Ca}^{2+}]_i$ concentrations in Jurkat cells which maintain a baseline $[\text{Ca}^{2+}]_i$ of approximately 100 nM [17]. The Ca^{2+} stored in organelles for signaling events is approximately 30–300 μM [18] and can be released in small amounts, triggering local cellular events, and/or generating Ca^{2+} waves [19,20]. Cell functions that are Ca^{2+} -mediated are dependent on varying spatial and temporal $[\text{Ca}^{2+}]_i$ concentrations. Examples of Ca^{2+} -mediated cell events include fertilization, muscle contraction, and apoptosis (programmed cell death) [17,21–23].

Applying nsPEFs increases $[\text{Ca}^{2+}]_i$ in a variety of cell types. A field strength-dependent synchronized response was first shown in Jurkat (lymphoid leukemia cell line) and HL-60 (myeloid leukemia cell line) cells [24,25]. It was concluded that both Ca^{2+} influx and intracellular release contributed to the observed transients. In HL-60 cells, a pulse-induced $[\text{Ca}^{2+}]_i$ increase mimicked a hormone-stimulated increase in $[\text{Ca}^{2+}]_i$, where the magnitude of the response was reduced in the absence of extracellular Ca^{2+} and the pulse-induced increase in $[\text{Ca}^{2+}]_i$ reached a peak in approximately 1 s [26].

Jurkat cells loaded with the Ca^{2+} sensitive fluorescent indicator Calcium Green showed increases in $[\text{Ca}^{2+}]_i$ after ten 30-ns pulses of 2.5 kV/cm [4]. The response was recorded with a resolution limit of

* Corresponding author. Tel.: +1 757 683 2414; fax: +1 757 314 2397.
E-mail address: jkolb@odu.edu (J.F. Kolb).

100 ms. The same cells did not lose membrane integrity as confirmed by the lack of propidium iodide uptake, which indicates that the increase in $[Ca^{2+}]_i$ was due to internal Ca^{2+} release rather than Ca^{2+} influx. The experiments so far suggest that in the presence of extracellular Ca^{2+} , the majority of the increase in $[Ca^{2+}]_i$ following nsPEF was due to Ca^{2+} influx. However, in the absence of extracellular Ca^{2+} , the increase in $[Ca^{2+}]_i$ was generated from intracellular Ca^{2+} stores, most likely by electroporation of intracellular membranes. The influx of Ca^{2+} from the extracellular medium is through non-specific nanopores in the plasma membrane [27] or through the opening of Ca^{2+} -release-activated-channels (CRAC) on the membrane (termed store-operated Ca^{2+} entry) [17].

Thus far, the temporal Ca^{2+} response to nsPEF exposures has been observed on a 100-ms time scale, which was not fast enough to allow observation of the initial Ca^{2+} release [4]. Within this time frame, it was also not possible to determine the source of the pulse-induced Ca^{2+} response. Only instantaneous and uniform increases in $[Ca^{2+}]_i$ across the entire cell volume were reported due to nsPEF stimulation [4]. Increasing the temporal and spatial resolution of $[Ca^{2+}]_i$ measurements will identify the location of the Ca^{2+} release and the underlying pathways behind the pulse-induced Ca^{2+} response. To this end, our study (1) investigated changes in $[Ca^{2+}]_i$ dependent upon field strength and the presence of extracellular Ca^{2+} , (2) resolved nsPEF-induced $[Ca^{2+}]_i$ responses, comparing the kinetics and magnitude to spontaneous $[Ca^{2+}]_i$ transients, and (3) determined the origin of the Ca^{2+} release site.

2. Methods

2.1. Cell culture

Jurkat cells obtained from American Type Culture Collection (ATCC, Manassas, VA) were cultured in 75-cm² flasks in RPMI 1640 medium (Mediatech Cellgro, Herndon, VA) supplemented with 10% fetal bovine serum (Atlanta Biologicals, Norcross, GA), L-glutamine (2.0 mM), penicillin (100 U/ml), streptomycin (100 µg/ml) (Mediatech Cellgro, Herndon, VA) and incubated at 37 °C with 5% CO₂. Cells in log-phase were removed from the culture and re-suspended in a modified Tyrode's buffer composed of 145.0 mM NaCl, 5.0 mM KCl, 0.4 mM NaH₂PO₄, 1.0 mM MgSO₄, 6.0 mM glucose, 5.0 mM HEPES (4-(2-Hydroxyethyl)-1-piperazineethanesulfonic acid) with or without 1.5 mM CaCl₂, and with enough NaOH to bring the pH to 7.4 [13]. The conductivity and osmolarity of the medium were 14.07 mS/cm and 285.5 mOsm respectively. In experiments with Ca^{2+} -free buffer, CaCl₂ was omitted from the suspension solution and 1.5 mM EGTA (Ethylene glycol-bis(beta-aminoethyl ether)-N,N,N',N'-tetraacetic acid) was added to chelate residual Ca^{2+} .

2.2. Cell staining

Cells were loaded with the Ca^{2+} fluorophore fluo-4, by incubating with 4 µM fluo-4, AM for 30 min. Excess un-hydrolyzed fluo-4, AM was removed by centrifuging the cell suspension at 50 ×g for 5 min and re-suspending the cells in fresh buffer. To locate the position of the endoplasmic reticulum, cells were stained with 1 µM brefeldin A, BODIPY® 558/568 for 30 min then centrifuged at 50 ×g for 5 min and re-suspended in fresh buffer. Cell membrane integrity was assessed by adding 10 µg/ml of propidium iodide before exposure to nsPEFs and measuring fluorescence after exposure using microscopy.

2.3. Pulse chamber

Electric field pulses were administered to cells between plane-parallel electrodes of 10 mm length, a depth of 10–15 µm, and a distance across the gap between the electrodes of 80 µm. The microcuvettes were provided to us by Dr. John Booske (Department

of Electrical Engineering, University of Wisconsin, Madison, WI). Electrodes were nickel-plated onto 1 × 3 × 0.04 in. microscope slides or no. 1–1/2 covers (22 × 50 mm) that were pre-coated with a 100 nm gold layer on top of a 5 nm adhesion layer. During electroplating, the gap was kept defined by a barrier of photoresist, which was deposited prior in a photolithographic process. The photoresist was subsequently removed by acetone and the remaining metal layers in the gap by a gold etchant and buffered hydrofluoric acid, respectively [28].

An aliquot of stained cells was pipetted between the 80 µm electrode gap. A coverslip was placed on the gap and the slide placed in the pulse chamber set up to deliver a square wave pulse, similar to that described previously [13]. We did not use any agent such as poly-L-lysine to fix the cells to the slide since the cells did not move during the time course of the experiments. The electrode thickness was approximately 15 µm and the diameter of a typical Jurkat cell is approximately 11.5 µm [29].

2.4. Experimental setup

A Blumlein line circuit was used to deliver 60-ns rectangular pulses with a rise time of 2–4 ns to cells in suspension [30]. The pulse generator and the confocal system were synchronized such that a delay generator (Berkeley Nucleonics BCN555, San Rafael, CA) initiated the start of time-lapse movie 10 s before the application of the first pulse. If a second pulse was applied, it was triggered by the delay generator 300 s later. For the application of a single pulse, this time was set to 10 s. The delay generator and image acquisition were controlled by a MATLAB (The MathWorks, Natick, MA) program.

2.5. Fluorescence microscopy and image analysis

Time-lapse images were recorded using the UltraVIEW Rapid Confocal Imager (Perkin Elmer, Waltham, MA), a spinning-disc, confocal microscope attached to an Olympus IX71 inverted microscope, capable of taking up to 360 frames per second. The confocal unit was connected to a computer with the Perkin Elmer UltraVIEW ERS software installed, which provides an interface between the excitation laser, camera controls, and the visual display. The Argon/Krypton ion laser (Melles Griot, Carlsbad, CA) 643-Y-AO2, attached to the system, lased at wavelengths 488, 568, and 647 nm. For experiments with a time scale of 1 s per frame with 100 ms exposure, a 60× long-pass air objective was used, but for the smaller time scale of 18 ms per frame with a 5-ms exposure, a 60× oil objective was used. Changes in fluorescence were derived for individual cells (region of interest) from the recorded grey-scale values with the analysis option of UltraVIEW ERS. For the statistical treatment, the results were treated with Microsoft Excel 2003 – Analysis ToolPak (Microsoft Corporation, Redmond, WA).

3. Results

3.1. Physiological $[Ca^{2+}]_i$ fluctuations

To characterize the dynamics of the $[Ca^{2+}]_i$ response to nsPEF exposure, Jurkat cells were stimulated with 60 ns duration pulses of either 25, 50, or 100 kV/cm field strength in the presence (left column) and absence (middle and right column) of extracellular Ca^{2+} (Fig. 1). Fluorescence intensity changes expressed in grey level were obtained for each cell in the field of view. The recordings were started before the exposure to capture a baseline fluorescence value for normalization and then continued for 10–15 min (Fig. 1). Control cells exhibited spontaneous surges (oscillations) in $[Ca^{2+}]_i$ in the presence or absence of extracellular Ca^{2+} (Fig. 1, panels A and B). As shown in Fig. 2, regardless of extracellular Ca^{2+} , the maximum increase in fluorescence reached values 1.35–1.40 fold above baseline values. The peak value was reached in approximately 4 s and $[Ca^{2+}]_i$ levels returned to values comparable to the initial signal within 1.5–

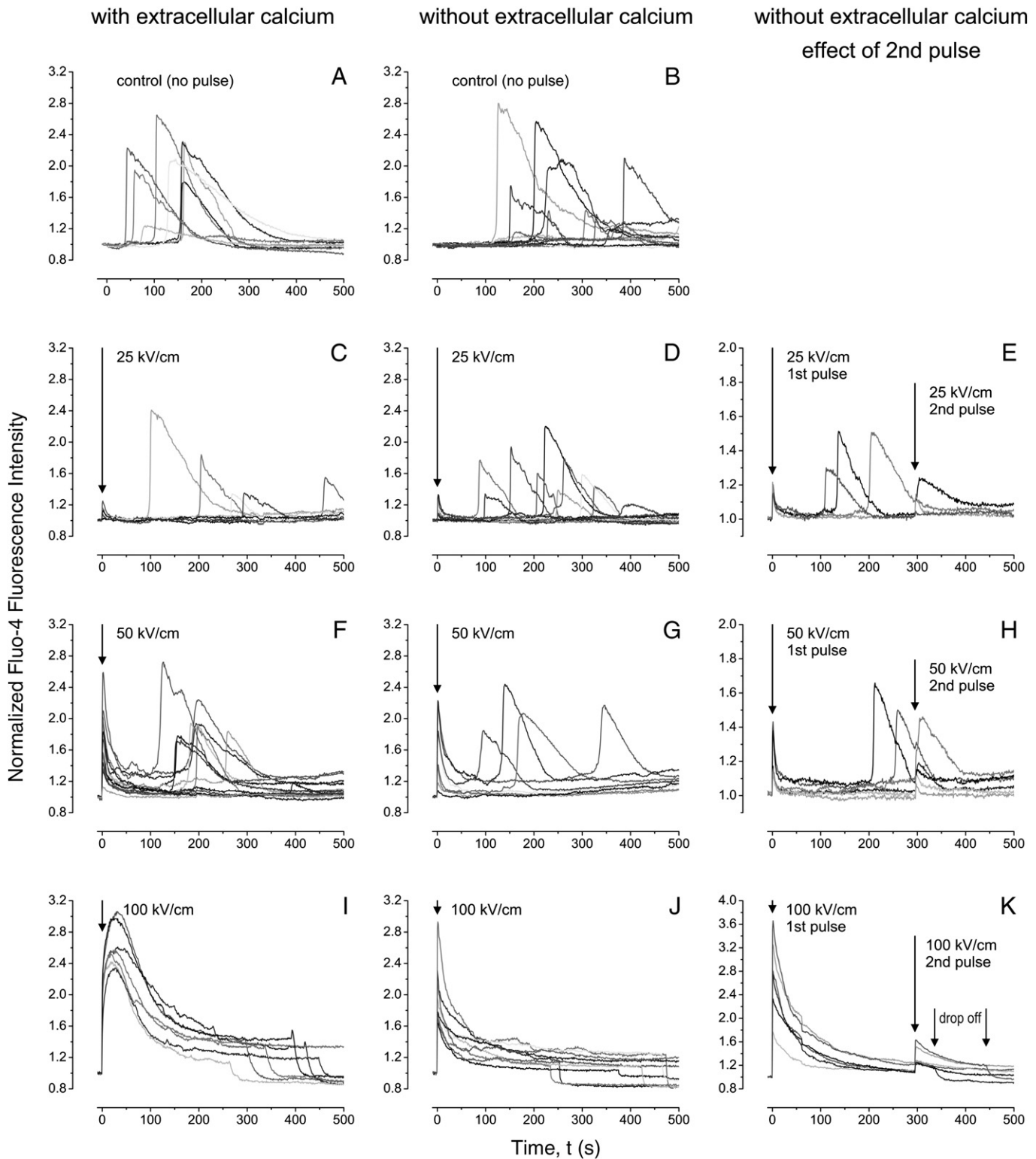


Fig. 1. Typical fluorescence recordings of fluo-4 loaded Jurkat cells stimulated with a 60-ns pulsed electric field. Images of cells were taken every second with a 100-ms exposure time and stimulated with a single pulse at the 10th second (first and second column), and then exposed to an additional pulse at the 300th second (third column). Individual responses vary greatly between cells. (Note considerable deviations from the averages shown in Fig. 2 for outliers in particular for the unstimulated responses of the control groups.)

5 min. The spontaneous response was characterized by an initial moderate increase in $[Ca^{2+}]_i$ as seen in Fig. 3A. Once the fluorescence signal reached about 10% of the peak value, the rate of change increased rapidly. The time from the onset of this steep rise until the maximum was reached is reported in Fig. 2.

Similar $[Ca^{2+}]_i$ transients lasting approximately 100 s, have been described [19,20]. Periodically, the fluorescence intensity, after falling to values around baseline, started to gradually increase again, although at a rate much slower than the initial rise (data not shown). Antigen receptor-stimulated release of inositol triphosphate

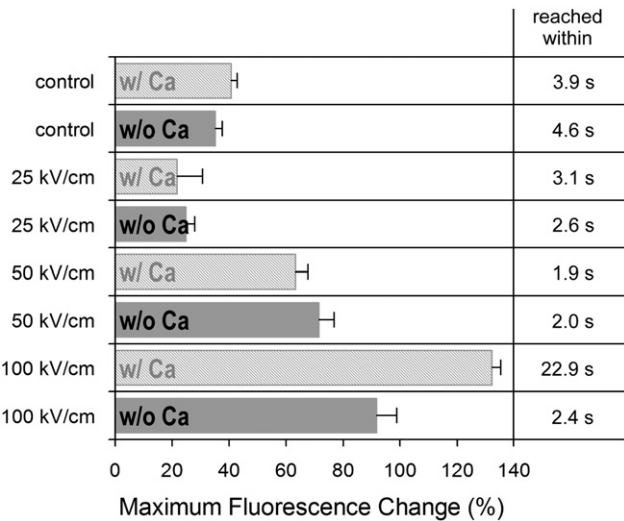


Fig. 2. Statistical analysis of average fluorescent signal magnitude (in percent above the baseline level) and time to reach this value from baseline values for recordings shown in Fig. 1. For the slow increase in the control groups, the time for the increase was determined as the time it took to reach the highest value from 10% of this value. In comparison, the increase of the response observed with nsPEF-stimulus occurred immediately within the limits of the temporal resolution. The data analysis is based on values from different experiments with at least 30 cells in total for each condition. The average response for different experiments was computed including only values within a confidence interval of two standard deviations. For 100 kV/cm the response in the presence of Ca^{2+} was statistically significantly stronger than without Ca^{2+} .

(IP_3) in Jurkat cells triggers oscillations in $[\text{Ca}^{2+}]_i$ [e.g. 31,32] with a slow rise similar to that shown in this study (Fig. 1).

3.2. Field strength dependent Ca^{2+} response

Cells exposed to an electric field of 12 kV/cm for 60 ns exhibited no measurable increase in $[\text{Ca}^{2+}]_i$ (data not shown). The application of 25 kV/cm or more led to an immediate increase in $[\text{Ca}^{2+}]_i$ in all exposed cells. For a 25 kV/cm field exposure the peak values were 1.25 times higher than the baseline value and were reached between 2.6 and 3.0 s following stimulation (Fig. 2). The fluorescence signal returned to values measured before the exposure in approximately 30 s. A dependency of the response on extracellular Ca^{2+} was not observed. Compared to the spontaneous response, the nsPEF stimulated response had a lower peak value, was reached in a shorter time, and was not preceded by a gradual increase.

Qualitatively, the response to 50 kV/cm was similar to the 25 kV/cm response however the peak was 1.7 times higher than baseline values. The maximum fluorescence response was reached 1.9–2.0 s after the pulse, which was slightly faster than measured with the lower field strength. No dependency on extracellular Ca^{2+} was observed. The fluorescence signal returned to baseline within 1 min, which was slower than the return using 25 kV/cm, but still much faster than the physiological spontaneous response. For 25 and 50 kV/cm conditions, the cells showed no lasting effect of the nsPEF exposure since their $[\text{Ca}^{2+}]_i$ levels returned to pre-pulse levels within several minutes.

The response to a 100 kV/cm pulse was distinctly different from the exposures at lower field strengths. In the presence of extracellular Ca^{2+} , cells exhibited a fast increase in fluorescence intensity within 2 s to values approximately twice as high as the baseline value. This rapid rise was followed by a more gradual increase and a maximum fluorescence value of 2.3 times above the baseline in 23 s. The slow secondary increase in fluorescence was then followed by an equally slow decrease. The fluorescence signal leveled off after several minutes, however, at values higher than baseline values. For most cells, the fluorescence signal then suddenly

dropped from this value in 30–60 s to values that were even lower than the initial baseline values. With extracellular Ca^{2+} present, almost every cell followed this pattern. The time at which cells suddenly lost fluorescence varied, and was observed as early as 3 min after nsPEF exposure. The sudden drop in fluorescence was usually preceded by a small spike in fluorescence.

In the absence of extracellular Ca^{2+} , the initial rapid increase in fluorescence was similar to the response of cells exposed to 100 kV/cm in the presence of extracellular Ca^{2+} . A peak value 1.9 times higher than the baseline level was reached in approximately 2.4 s. However, this peak value was not followed by a further gradual increase. Consequently the maximum fluorescence changes in the presence and absence of extracellular Ca^{2+} for the 100 kV/cm field exposure were significantly different from each other (Fig. 2). The subsequent decrease in fluorescence intensity was again similar for both conditions. In this process, occasionally, the fluorescence intensity of individual cells dropped to values below the pre-exposure values after several minutes. The drop took about 15–20 s in the absence of Ca^{2+} and 2–3 times longer in its presence. In the latter case it was preceded by a small spike in fluorescence.

Another distinct difference observed only for exposures of 100 kV/cm was the absence of any spontaneous physiological response following the pulse induced response. When a second pulse of the same field strength was applied, 5 min after the first exposure (Fig. 1,

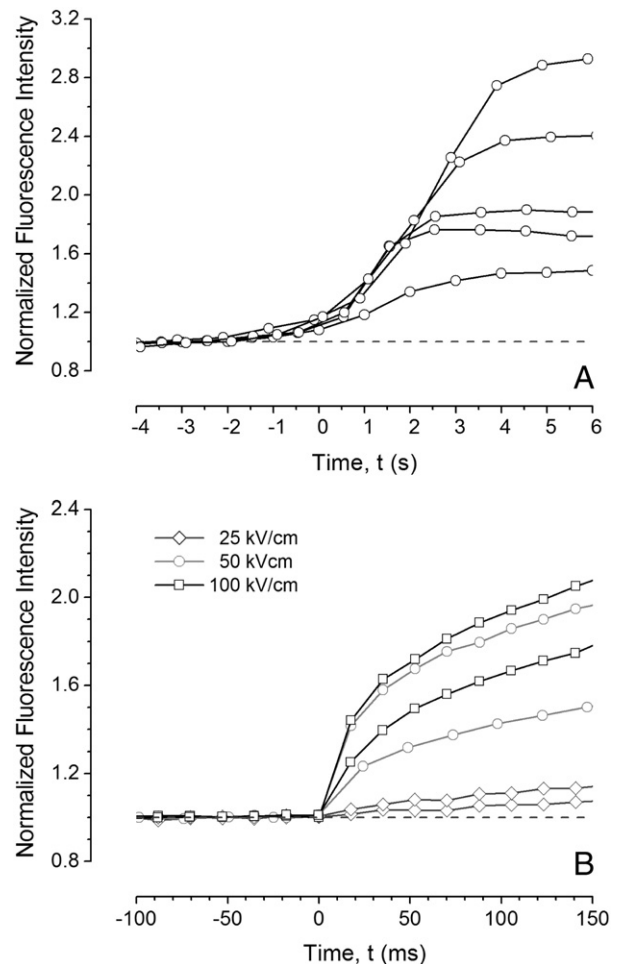


Fig. 3. In panel A, the time course for the spontaneous increases in $[\text{Ca}^{2+}]_i$ is shown for 5 representative cells. In panel B, the time course for the increase in $[\text{Ca}^{2+}]_i$ induced by 25, 50, and 100 kV/cm pulses is shown for two representative cells at each voltage. The response to the application of a 60-ns pulsed electric field was recorded taking images every 18 ms with an exposure time of 5 ms per image. The time scales between panels A and B differ by a factor of forty.

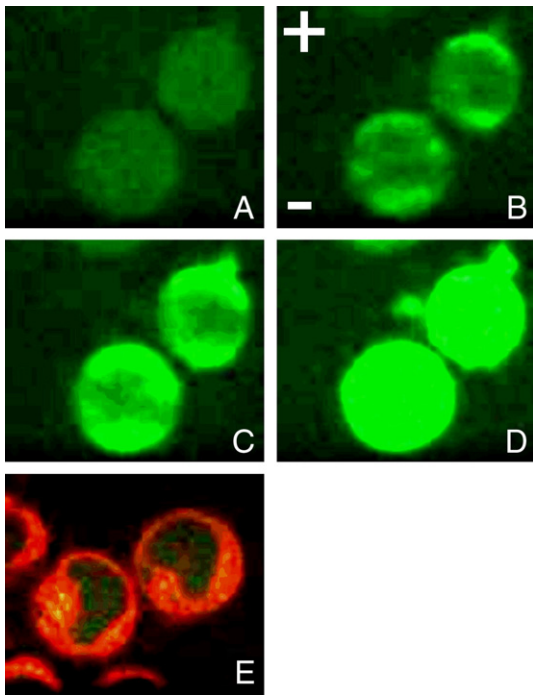


Fig. 4. Jurkat cells loaded with fluo-4 were imaged every 18 ms with a 5-ms exposure after exposure to a 60-ns pulse of 100 kV/cm (panel A). Image A was taken before exposure. Image B was taken at 18 ms, Image C at 36 ms and Image D at 54 ms. Cells were stained with brefeldin A, BODIPY[®] 558/568 to locate the endoplasmic reticulum (Image E).

right column), even for cells exposed to 100 kV/cm another increase in $[Ca^{2+}]_i$ was observed. Experiments with a second pulse were conducted in the absence of extracellular Ca^{2+} only, and for all conditions, the second response was lower in magnitude. For lower field strengths, the normal spontaneous behavior of the cell was unchanged by subsequent exposures, but was absent after the application of a subsequent 100-kV/cm pulse. Furthermore, the likelihood of the fluorescence signal to drop suddenly after exposure increased with the number of pulses applied. For the condition where 5 pulses were applied within 10 s, every cell showed a drop in fluorescence within a few minutes (data not shown).

3.3. Kinetics of nsPEF induced $[Ca^{2+}]_i$ response

The increases in $[Ca^{2+}]_i$ levels following the application of nsPEFs were previously reported as occurring “as fast as they can be observed”, which was defined by a temporal resolution of 100 ms [4]. However, recent simulation studies predict the release of Ca^{2+} from internal stores through pulse-induced pores, reaching saturation thresholds in a few microseconds [33]. To further define the mechanisms leading to increased $[Ca^{2+}]_i$ after the exposure to nsPEFs, we enhanced the temporal resolution. Time-lapse movies were recorded with a 5-ms exposure every 18 ms for 5 s. The pulse generator and the recording software were synchronized and a pulse was applied 1 s after recording had started. The experiments were conducted in the absence of extracellular Ca^{2+} . The traces in Fig. 3A show, on an expanded time scale, several individual cell fluorescence signals in control cells similar to the traces presented in Fig. 1B. Each of the data points, taken 1 s apart, represents the fluorescence value collected for a camera exposure of 100 ms. For graphical presentation, the individual signals were shifted in time from their original recording and overlaid, with time zero defined as the time when they have reached 10% of their maximum value. It typically took several seconds until the fluorescence signal increased to this value from baseline. Following this slow onset, the rate of the fluorescence

change rapidly increased, but it still took approximately 4 s to reach the peak value (Fig. 2). In comparison, the pulse induced responses were much faster. Examples of responses to different applied electric fields are shown in Fig. 3B, note that the time interval shown in panel B is forty times shorter than the one shown in panel A. A slow rise, as observed with the physiological responses, was not observed. For the applications of 50 kV/cm and 100 kV/cm fields, the signal increased 1.2 times higher than baseline values within approximately 36 ms. Physiological responses took 5000 times longer (3–4 s) to reach similar fluorescence values. Although the rate of fluorescence change was different for a field strength of 25 kV/cm, compared to the higher electric field strengths, it was not significantly different from the slow rise of a physiological response. Altogether, these results demonstrate that a 60 ns pulse with an electric field amplitude at or above 50 kV/cm stimulates a much faster Ca^{2+} response than any physiological stimulus.

3.4. Origin of pulse induced increase in $[Ca^{2+}]_i$

A series of images taken with a 5 ms exposure every 18 ms allowed us to spatially resolve the increase in Ca^{2+} concentrations and identify potential intracellular sources. Previous studies were only able to report a homogeneous increase throughout the cell [4]. Staining with the fluorescence indicator brefeldin A, BODIPY[®] 558/568 [34] indicates the location of the endoplasmic reticulum (ER) (Fig. 4, panel E). In the absence of extracellular Ca^{2+} , there was an increase in $[Ca^{2+}]_i$ emanating from the site of the ER at the poles of the cells i.e. along the direction of the electric field. The poles were affected first and more intensely than the equatorial plane. The staining of the ER was co-localized with the fluo-4 fluorescence increase observed after nsPEF stimulation. Subsequently, the fluorescence intensity increased across the cell reaching homogeneous levels within 54 ms (Fig. 4, panel D). In comparison, recordings of spontaneous Ca^{2+} signals with the same fast resolution show a gradual and even increase throughout the cell, over a longer period of time, with no specific localization for the origin of the Ca^{2+} signal (data not shown).

3.5. Fluo-4 fluorescence response and membrane integrity

The sudden drop in fluorescence levels observed after the exposure to 100 kV/cm, independent of the presence of extracellular Ca^{2+} (Fig. 1I and J), indicated a loss of membrane integrity. Cells loaded with fluo-4 and exposed, in the presence of extracellular propidium iodide (PI), to 60-ns pulses of 100 kV/cm did not show an

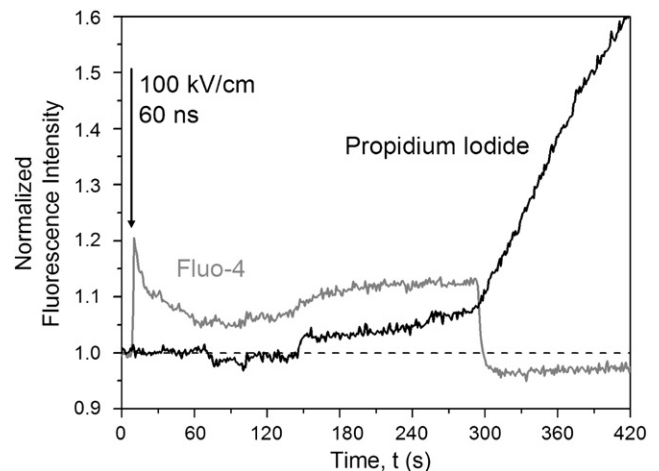


Fig. 5. Jurkat cells loaded with fluo-4 were exposed to a 60-ns pulsed electric field of 100 kV/cm in the presence of extracellular Ca^{2+} and the membrane integrity marker propidium iodide.

immediate uptake of this otherwise membrane impermeant dye (Fig. 5). However, when a sudden drop in the fluo-4 fluorescence was observed, PI was observed to be simultaneously and rapidly taken up by the cell (Fig. 5). In the presence of extracellular Ca^{2+} , this delayed rapid decrease was typical for almost every cell after the application of only one pulse. In the absence of extracellular Ca^{2+} , up to five pulses in close succession of 1 to 2 s had to be applied to observe this rapid drop in fluo-4 signal (data not shown). In short, whenever this fluorescence decrease occurred, simultaneous uptake of PI was always observed.

4. Discussion

The data presented show that the nsPEF-induced increase in $[\text{Ca}^{2+}]_i$ is an immediate, electric field strength-dependent, response (Fig. 1). The presence or absence of extracellular Ca^{2+} was irrelevant for responses to electric fields of 25 and 50 kV/cm (Fig. 2). The signal rises faster to its peak value than for the spontaneous $[\text{Ca}^{2+}]_i$ responses and also decreased faster to baseline values. After nsPEF exposure, normal fluctuations in $[\text{Ca}^{2+}]_i$ occurred again. The cell response was different for a field of 100 kV/cm when compared to lower field strengths and with respect to the presence of extracellular Ca^{2+} . Without extracellular Ca^{2+} , the initial signal was similar to the response for lower fields. However, $[\text{Ca}^{2+}]_i$ levels did not return to baseline values and no further increase above this value could be observed unless a second, similar pulse was applied. The $[\text{Ca}^{2+}]_i$ rise in the presence of extracellular Ca^{2+} reached a considerably higher peak level much later. Another characteristic of the response to the 100-kV/cm stimulus was a delayed (within 15 min) fast drop in fluo-4 fluorescence, which could be seen for almost every cell when extracellular Ca^{2+} was present, and also for some cells when extracellular Ca^{2+} was absent.

The $[\text{Ca}^{2+}]_i$ response, observed in the absence of external Ca^{2+} and for lower electric fields of 25 and 50 kV/cm, suggests that Ca^{2+} was released from internal stores. For 25 kV/cm a second pulse seemed to lead to amplitudes that were only slightly lower than for the first exposure. However, a second pulse of 50 kV/cm was not followed by the same increase as the first. This result indicates an inability to release more Ca^{2+} upon this second stimulus, either because the cell had become less sensitive to the exposure, or Ca^{2+} stores were depleted. This threshold seems to be overcome by increasing the field strength to 100 kV/cm. The significantly larger signal amplitude, in the presence of extracellular Ca^{2+} , was caused by the influx of Ca^{2+} . This hypothesis was supported by the slower increase to this higher value, which followed the initial rapid development similar to the response observed with no extracellular Ca^{2+} . How Ca^{2+} entered the cell is not completely understood. A likely explanation is that nsPEF causes the formation of nanopores which are large enough to allow Ca^{2+} to enter the cell but are too small for the uptake of larger molecules such as PI [27,35] or for fluo-4 to flow through. In our experiments, no observed increase in PI fluorescence while intracellular fluo-4 signals were high, supports this explanation (Fig. 4B). Conversely, the uptake of PI several minutes after 100 kV/cm nsPEF exposure correlated well with a sharp decrease in fluo-4 fluorescence below baseline levels, indicating that large pores had opened in the membrane as a secondary response to the exposure (Fig. 4B). Efflux from the cell and dilution of fluo-4 in the large extracellular volume would account for the decline in fluorescence signal. The lack of spontaneous fluctuations in $[\text{Ca}^{2+}]_i$ observed after the pulse at this field strength indicates that there was significant damage to the cell that prohibited normal Ca^{2+} homeostasis events to occur.

We recognize the possibility that the presence of EGTA in the low Ca^{2+} condition may lessen the ability of nsPEF to electroporate the plasma membrane. Chelators have been shown to alter the stability and rigidity of membranes (this is based on studies performed in red blood cells) [36]. However, since we still observe nsPEF induced increases in $[\text{Ca}^{2+}]_i$ in the EGTA condition, this implies that the nsPEF is affecting intracellular Ca^{2+} stores. Even if there was no electro-

poration of the plasma membrane in the EGTA condition this would not influence our results. Studies in our laboratory showed that by using patch clamp techniques, the permeabilization of GH3, PC-12 and Jurkat cells was not influenced by 10 mM EGTA [14].

In addition to nanopores allowing the influx of Ca^{2+} following nsPEF-stimulation, an alternative pathway for Ca^{2+} entry could be the activation of Ca^{2+} -release-activated-channels (CRAC) in the plasma membrane. This could be achieved with field strengths of 100 kV/cm which are large enough to trigger capacitive Ca^{2+} entry through the initial release of Ca^{2+} from internal stores [26,37]. The results for lower field strengths show that the electric fields were affecting internal stores and leading to increased $[\text{Ca}^{2+}]_i$. The endoplasmic reticulum was expected to be the most likely source for this Ca^{2+} increase and our fast time resolution images support this assumption (Fig. 4A).

Spontaneous increases in $[\text{Ca}^{2+}]_i$ took approximately 4 s to reach a maximum and consequently could easily be resolved with an image taken every 18 ms. It is obviously a response, with extracellular Ca^{2+} present, that involves the opening of Ca^{2+} channels in the plasma membrane, which are known to occur on the order of milliseconds [38]. In comparison, the initial temporal response of the pulse-induced Ca^{2+} release was found to occur much faster. The change in $[\text{Ca}^{2+}]_i$ for cells pulsed at 50 and 100 kV/cm showed a fast rise to values comparable to spontaneous oscillation peak amplitudes within the first 100 ms of exposure (often within 2–3 frames, i.e., 54 ms). Even on this time scale, the onset of the increase appears to be instantaneous with no indication of a gradual activation of ion channels. For 25 kV/cm the increase in $[\text{Ca}^{2+}]_i$ was too slow to allow us to determine with statistical significance if the induced response differs from the response of cells in the control. This suggests that either a fast rise in Ca^{2+} is triggered in less than 18 ms, or fluo-4 cannot bind quickly enough to the pulse-mobilized Ca^{2+} , although fluo-4 operates within milliseconds [39].

These results suggest that the mechanism by which nsPEFs induce increases in $[\text{Ca}^{2+}]_i$ may not be mediated by IP_3 and may not be following a physiological pathway. However, a contribution to increased $[\text{Ca}^{2+}]_i$ from internal stores through directly activated channels cannot be excluded. Recent experimental results and simulations suggest that an instantaneous and substantial increase in $[\text{Ca}^{2+}]_i$ observed on a millisecond timescale is caused by the formation of pores. These pores form as a result of rapid changes in membrane potentials that surpass the membrane threshold due to applied high electric fields [27,40]. For the plasma membrane, changes in membrane potential values of more than 1 V have been observed within a few nanoseconds into the application of a 60 ns pulsed electric field of 100 kV/cm [13]. The voltage across the membrane rises further, to values of 1.4 V, in 20 ns before it gradually decreases. The decrease has been associated with the exchange of ions across the membrane. Since the pulse duration is much shorter than the charging time of the cell, the interior of the cell is not yet shielded from the external field and organelle membranes are charged in a manner similar to the outer membrane [41,42]. In fact, for their smaller size and higher membrane curvature, they are expected to be even easier to porate [43]. We therefore believe that Ca^{2+} is released from the endoplasmic reticulum through pores that were formed during the application of the electric field. Differences in amplitudes of the $[\text{Ca}^{2+}]_i$ signals for different field strengths can be explained as a result of different pore densities. This initial process might also trigger the eventual opening of CRAC channels. The hypothesis of pores enabling the outflow of Ca^{2+} is further supported by the observed initial release from the endoplasmic reticulum compartment at the poles (Fig. 4B). Stronger or initial effects along the direction of the electric field are also known for electroporation pulses [8,44,45], and in this case are ascribed to the highest values of membrane potential changes where the electric field is perpendicular to the membrane surface. This typically results in the formation of pores. The similarity

of this trend with our experiments suggests that with the 60-ns pulse, the applied electric field reaches into the cell and that pores are formed at an internal membrane, most likely the ER. This may allow for the passage of Ca^{2+} , which we observe as an increase in fluo-4 fluorescence intensity. Also, the pulse induced Ca^{2+} release generally shows a faster and more exponential decline, rather than a linear decrease, back to baseline values as seen with the spontaneous increases (e.g. Fig. 1F and G), which suggests some mechanism other than the mere opening and closing of Ca^{2+} channels.

The creation of pores in the outer membrane also seems to be the primary process for the uptake of Ca^{2+} from the external medium. Evidence for the formation of pores in Jurkat cells, following nsPEF treatment, was previously obtained when the influx of YO-PRO-1 was observed along with externalization of phosphatidylserine [3]. At the same time, no PI entered the cells, which supports the theory that these pores are different than those induced by electroporation pulses, in particular, that they are much smaller and can discriminate between dyes with similar molecular weights. PI has a Connolly solvent exclusion volume of 394 \AA^3 which is slightly larger than YO-PRO-1 which is 355 \AA^3 (calculated using Chem 3D Ultra version 8.0.3, CambridgeSoft Corp, Cambridge, MA), which may be a sufficient difference to account for their different permeabilities through nanopores. Influx of Ca^{2+} through nanopores in the plasma membrane together with the outflow of Ca^{2+} from internal stores appears adequate to activate CRAC channels on the plasma membrane. We believe that this can be seen in the further 45% increase in $[\text{Ca}^{2+}]_i$ when extracellular Ca^{2+} was present (Fig. 11) from a $[\text{Ca}^{2+}]_i$ value at 2.0 s, which was similar to the maximum seen without extracellular Ca^{2+} at 2.4 s (Fig. 1J), to a peak level which was slowly reached at 22.9 s (Fig. 2).

In conclusion, our results confirm modeling results that predict, for the exposure to nanosecond pulsed electric fields with field strengths of several tens of kilovolts per centimeter, the formation of pores in the plasma and also internal membranes [27,35]. These 'nanopores' are too small for larger molecules, such as PI, to pass through but permit passage of smaller ions like Ca^{2+} . Longer electrical pulses have been shown to produce primarily large pores in the plasma membrane that will permit the introduction of big molecules such as DNA into cells. However, organelles can be affected as well. Electrical field pulses of 50- μs duration were shown to produce reversible breakdown of plasma membrane and tonoplast membranes as judged by the influx of extracellular Ca^{2+} and the release of tonoplast Ca^{2+} in aequorin-transformed tobacco cells [46].

For nsPEFs of different pulse durations and field strengths, combined with multiple exposures, our data suggests the possibility of activating specific cell responses, such as the expression of interleukin-2 in Jurkat cells. To this end, it would be of interest to observe the long-term effects of exposures. For certain pulsed electric field parameters the induction of apoptosis has already been demonstrated [47]. Based on our research, the ability to trigger other Ca^{2+} controlled responses is likely. For platelets this response has already been exploited as non-ligand agonist for activation [48]. Therefore, nsPEF stimulation offers a subtle tool to manipulate Ca^{2+} pathways to obtain a specific desired event. By varying nsPEF exposures (both energy and pulse duration), it may be possible to selectively stimulate cell proliferation, expression of interleukin-2, or apoptosis, by increasing $[\text{Ca}^{2+}]_i$ to different levels. The regulation of these processes may ultimately offer new treatment possibilities for selected medical conditions and, in particular, may open the door to new cancer treatments, for example, by specifically inducing Ca^{2+} mediated apoptosis in tumor cells [49].

Acknowledgements

This study was funded by an AFOSR DOD MURI grant on "Subcellular Response to Narrow Band and Wide Band Radio Frequency Radiation" administered by Old Dominion University.

References

- [1] K.H. Schoenbach, R.P. Joshi, J.F. Kolb, N. Chen, M. Stacey, P.F. Blackmore, E.S. Buescher, S.J. Beebe, Ultrashort electric pulses open a new gateway into biological cells, *Proc. IEEE* 92 (2004) 1122–1137.
- [2] K.H. Schoenbach, S.J. Beebe, E.S. Buescher, Intracellular effect of ultrashort electrical pulses, *Bioelectromagnetics* 22 (2001) 440–448.
- [3] P.T. Vernier, M.J. Ziegler, Y. Sun, W.V. Chang, M.A. Gundersen, D.P. Tieleman, Nanopore formation and phosphatidylserine externalization in a phospholipid bilayer at high transmembrane potential, *J. Am. Chem. Soc.* 128 (2006) 6288–6289.
- [4] P.T. Vernier, Y. Sun, L. Marcu, S. Salemi, C.M. Craft, M.A. Gundersen, Calcium bursts induced by nanosecond electric pulses, *Biochem. Biophys. Res. Commun.* 310 (2003) 286–295.
- [5] M. Stacey, J. Stickley, P. Fox, V. Statler, K. Schoenbach, S.J. Beebe, S. Buescher, Differential effects in cells exposed to ultra-short, high intensity electric fields: cell survival, DNA damage, and cell cycle analysis, *Mutat. Res.* 542 (2003) 65–75.
- [6] S.J. Beebe, J. White, P.F. Blackmore, Y. Deng, K. Somers, K.H. Schoenbach, Diverse effects of nanosecond pulsed electric fields on cells and tissues, *DNA Cell Biol.* 22 (2003) 785–796.
- [7] J. Zhang, P.F. Blackmore, B.Y. Hargrave, S. Xiao, S.J. Beebe, K.H. Schoenbach, Nanosecond pulse electric field (nanopulse): a novel non-ligand agonist for platelet activation, *Arch. Biochem. Biophys.* 471 (2008) 240–248.
- [8] E. Neumann, S. Kakorin, K. Toensing, Fundamentals of electroporative delivery of drugs and genes, *Bioelectrochem. Bioenerg.* 48 (1999) 3–16.
- [9] U. Zimmerman, U. Friedrich, H. Mussauer, P. Gessner, K. Hamel, V. Sukhorukov, Electromanipulation of mammalian cells: fundamentals and application, *IEEE Trans. Plasma Sci.* 28 (2000) 72–82.
- [10] J.C. Weaver, Y.A. Chizmadzhev, Theory of electroporation: a review, *Bioelectrochem. Bioenerg.* 41 (1996) 135–160.
- [11] A.J.H. Sale, W.A. Hamilton, Effects of high electric fields on microorganisms. I. Killing of bacteria and yeasts, *Biochim. Biophys. Acta* 148 (1967) 781–788.
- [12] K.S. Cole, Electric impedance of marine egg membranes, *Trans. Faraday Soc.* 33 (1937) 972–996.
- [13] W. Frey, J.A. White, R.O. Price, P.F. Blackmore, R.P. Joshi, R. Nuccitelli, S.J. Beebe, K.H. Schoenbach, J.F. Kolb, Plasma membrane voltage changes during nanosecond pulsed electric field exposure, *Biophys. J.* 90 (2006) 3608–3615.
- [14] A.G. Pakhomov, J.F. Kolb, J.A. White, R.P. Joshi, S. Xiao, K.H. Schoenbach, Long-lasting plasma membrane permeabilization in mammalian cells by nanosecond pulsed electric field (nsPEF), *Bioelectromagnetics* 28 (2007) 655–663.
- [15] A.G. Pakhomov, R. Shevin, J.A. White, J.F. Kolb, O.N. Pakhomova, R.P. Joshi, K.H. Schoenbach, Membrane permeabilization and cell damage by ultrashort electric field shocks, *Arch. Biochem. Biophys.* 465 (2007) 109–118.
- [16] R.S. Lewis, Calcium signaling mechanism in T lymphocytes, *Annu. Rev. Immunol.* 19 (2001) 497–521.
- [17] A.B. Parekh, J.W. Putney, Store-operated calcium channels, *Physiol. Rev.* 85 (2005) 757–810.
- [18] B.D. Gomperts, I.M. Kramer, P.E.R. Tatham, Calcium and signal transduction, *Signal Transduction*, Academic Press, London, 2002, pp. 145–169.
- [19] M.J. Berridge, P.H. Cobbold, K.S. Cuthbertson, Spatial and temporal aspects of cell signalling, *Philos. Trans. R. Soc. Lond., B Biol. Sci.* 320 (1988) 325–343.
- [20] M.J. Berridge, A. Galione, Cytosolic calcium oscillators, *FASEB J.* 2 (1988) 3074–3082.
- [21] E. Carafoli, Calcium signalling: a tale for all seasons, *Proc. Natl. Acad. Sci.* 99 (2002) 1115–1122.
- [22] M.J. Berridge, M.D. Bootman, H.L. Roderick, Calcium signaling: dynamics, homeostasis and remodeling, *Nat. Rev., Mol. Cell Biol.* 4 (2003) 517–529.
- [23] S. Feske, Calcium signaling in lymphocyte activation and disease, *Nat. Rev., Immunol.* 7 (2007) 690–702.
- [24] E.S. Buescher, R.R. Smith, K.H. Schoenbach, Signaling without signals: submicrosecond intense pulsed electric field applications trigger rises in intracellular free Ca^{2+} concentration in cells, *Conf. Record 3rd International Symposium on Nonthermal Medical/Biological Treatments Using Electromagnetic Fields and Ionized Gases (Electromed)*, San Antonio, Texas, June 11–13 (2003) 47–48.
- [25] E.S. Buescher, R.R. Smith, K.H. Schoenbach, Submicrosecond intense pulsed electric fields on intracellular free calcium mechanism and effects, *IEEE Trans. Plasma Sci.* 32 (2004) 1563–1572.
- [26] J.A. White, P.F. Blackmore, K.H. Schoenbach, S.J. Beebe, Stimulation of capacitative calcium entry in HL-60 cells by nanosecond pulsed electric fields, *J. Biol. Chem.* 279 (2004) 22964–22972.
- [27] T.R. Gowrishanker, A.T. Esser, Z. Vasilkoski, K.C. Smith, J.C. Weaver, Microdosimetry for conventional and supra-electroporation in cells with organelles, *Biochem. Biophys. Res. Commun.* 341 (2006) 1266–1276.
- [28] S.M. Kennedy, Z. Ji, J.C. Hedstrom, J.H. Booske, S.C. Hagness, Quantification of electroporative uptake kinetics and electric field heterogeneity effects in cells, *Biophys. J.* 94 (2008) 5018–5027.
- [29] M.J. Rosenbluth, W.A. Lam, D.A. Fletcher, Force microscopy of nonadherent cells: a comparison of leukemia cell deformability, *Biophys. J.* 90 (2006) 2994–3003.
- [30] J.F. Kolb, S. Kono, K.H. Schoenbach, Nanosecond pulsed electric field generators for the study of subcellular effects, *Bioelectromagnetics J.* 27 (2006) 172–187.
- [31] S. Kunerth, G.W. Mayr, F. Koch-Nolte, A.H. Guse, Analysis of subcellular calcium signals in T-lymphocytes, *Cell. Signal.* 15 (2003) 783–792.
- [32] J. Galvanovskis, J. Sandblom, B. Bergquist, S. Galt, Y. Hammerius, Cytoplasmic Ca^{2+} oscillations in human leukemia T-cells are reduced by 50 Hz magnetic fields, *Bioelectromagnetics* 20 (1999) 269–276.

- [33] R.P. Joshi, A. Nguyen, V. Sridhara, Q. Hu, R. Nuccitelli, S.J. Beebe, J. Kolb, K.H. Schoenbach, Simulations of intracellular calcium release dynamics in response to a high-intensity ultrashort electric pulse, *Phys. Rev. E* 75 (2007) 041920–1–041920-10.
- [34] Y. Deng, J.R. Bennink, H.C. Kang, R.P. Haugland, J.W. Yewdell, Fluorescent conjugates of brefeldin A selectively stain the endoplasmic reticulum and Golgi complex of living cells, *J. Histochem. Cytochem.* 43 (1995) 907–915.
- [35] Q. Hu, R.P. Joshi, K.H. Schoenbach, Simulations of nanopore formation and phosphatidylserine externalization in lipid membranes subjected to a high-intensity, ultrashort electric pulse, *Phys. Rev., E Stat. Nonlinear Soft Matter Phys.* 72 (2005) 031902–1–031902-10.
- [36] H. Mussauer, V.L. Sukhorukov, A. Haase, U. Zimmermann, Resistivity of red blood cells against high-intensity, short-duration electric field pulses induced by chelating agents, *J. Membr.Biol.* 170 (1999) 121–133.
- [37] M. Vig, J.P. Kinet, The long and arduous road to CRAC, *Cell Calcium* 42 (2007) 157–162.
- [38] D.D. Friel, H.J. Chiel, Calcium dynamics: analyzing the Ca^{2+} regulatory network in intact cells, *Trends Neurosci.* 31 (2007) 1–19.
- [39] J. Xu, X. Wang, B. Ensign, M. Li, L. Wu, A. Guia, J. Xu, Ion-channel assays technologies: quo vadis? *Drug Discov. Today* 6 (2001) 1278–1287.
- [40] Q. Hu, S. Viswanadham, R.P. Joshi, K.H. Schoenbach, S.J. Beebe, P.F. Blackmore, Simulation of transient membrane behavior in cells subjected to a high-intensity ultrashort electric pulse, *Phys. Rev. E* 71 (2005) 031914–1–031914-9.
- [41] K.H. Schoenbach, B. Hargrave, R.P. Joshi, J.F. Kolb, R. Nuccitelli, C. Osgood, A. Pakhomov, M. Stacey, R.J. Swanson, J.A. White, S. Xiao, J. Zhang, S.J. Beebe, P.F. Blackmore, E.S. Buescher, Bioelectric effects of intense nanosecond pulses, *IEEE Trans. Dielectr. Electr. Insul.* 14 (2007) 1088–1109.
- [42] T. Kotnik, D. Miklavcic, Theoretical evaluation of voltage inducement on internal membranes of biological cells exposed to electric fields, *Biophys. J.* 90 (2006) 480–491.
- [43] S. Kakorin, E. Redeker, E. Neumann, Electroporative deformation of salt filled lipid vesicles, *Eur. Biophys. J.* 27 (1998) 43–53.
- [44] E. Tekle, H. Oubrahim, S.M. Dzekunov, J.F. Kolb, K.H. Schoenbach, P.B. Chock, Selective field effects on intracellular vacuoles and vesicle membranes with nanosecond electric pulses, *Biophys. J.* 89 (2005) 274–284.
- [45] M. Hibino, H. Itoh, K. Kinoshita, Time course of cell electroporation as revealed by submicrosecond imaging of transmembrane potential, *Biophys. J.* 64 (1993) 1789–1800.
- [46] V.L. Sukhorukov, J.M. Endter, D. Zimmermann, R. Shirakashi, S. Fehrmann, M. Kiesel, R. Reuss, D. Becker, R. Hedrich, E. Bamberg, Th. Roitsch, U. Zimmermann, Mechanisms of electrically mediated cytosolic Ca^{2+} transients in aequorin-transformed tobacco cells, *Biophys. J.* 93 (2007) 3324–3337.
- [47] S.J. Beebe, P.M. Fox, L.J. Rec, K. Somers, R.H. Stark, K.H. Schoenbach, Nanosecond, high-intensity pulsed electric fields induce apoptosis in human cells, *FASEB J.* 11 (2003) 1493–1495.
- [48] J. Zhang, P.F. Blackmore, B.Y. Hargrave, S. Xiao, S.J. Beebe, K.H. Schoenbach, Nanosecond pulse electric field (nanopulse): a novel non-ligand agonist for platelet activation, *Arch. Biochem. Biophys.* 471 (2008) 240–248.
- [49] R. Nuccitelli, U. Pliquett, X. Chen, W. Ford, J.R. Swanson, S.J. Beebe, J.F. Kolb, K.H. Schoenbach, Nanosecond pulsed electric fields cause melanomas to self-destruct, *Biochem. Biophys. Res. Commun.* 343 (2006) 351–360.